Ars Separatoria Acta 1 (2002) 111-137

ARS SEPARATORIA ACTA

www.ars_separatoria.chem.uni.torun.pl

AN ADSORPTION OF BOVINE SERUM ALBUMIN ON CARBON/ZIRCONIUM OXIDE MICROFILTRATION MEMBRANES AT DIFFERENT pH'S AS DETERMINED FROM BREAKTHROUGH CURVES

T. BIALOPIOTROWICZ[1*], P. BLANPAIN[2], F. RENÉ[3] and M. LALANDE[2]

[1] Maria Curie-Sklodowska University, Department of Physical Chemistry, Maria Curie-Sklodowska Sqr. 3, 20-031 Lublin, Poland
[2] Institut National de la Recherche Agronomique, Laboratoire de Génie des Procédés et Technologie Alimentaires, 369 rue Jules Guesde, BP 39, 59651 Villeneuve d'Ascq Cedex, France
[3] Institut National de la Recherche Agronomique, Laboratoire de Génie et Microbiologie des Procédés Alimentaires, CBAI - INA-PG, 78850 Thiverval Grignon, France

ABSTRACT

Adsorption of bovine serum albumin (BSA) at different pHs on carbon supported microfiltration (MF) inorganic membranes was measured by using breakthrough (BT) curves derived from liquid frontal chromatography. Adsorption was quantified in the presence of permeation through the membrane thickness at a constant flow rate. Using the method described, it was confirmed that BSA adsorption is dependent on pH and its maximum is near the BSA isoelectric point (i.e. pH 4.9). Using Langmuir's equation, monolayer capacities were determined. It was found that adsorption is of monomolecular type. Analysis of the methods (called algorithms) used for adsorption calculation was carried out. Monolayer capacities found were generally lower than theoretical BSA monolayer capacity in side-on orientation. It was concluded that such effects as pore blocking, deposition of aggregates inside the membrane or slow formation of dimers were not the main mechanisms of BSA uptake by the MF membranes studied during BT curve formation.

Keywords : BSA adsorption; inorganic membranes; breakthrough curve

* Corresponding author

INTRODUCTION

One very promising technique for colloidal suspension separation is cross-flow microfiltration (CFMF) [1]. Until now, the successful application of CFMF has been limited to replacement of conventional filtration. However, it is potentially very useful in some processes encountered in the food industry such as wine, beer and vinegar filtration [1,2]. In the dairy industry, bacteria removal from milk and whey and the separation of phosphocaseinate from milk and phospholipids and casein fines from whey are very promising [2]. The major applications of membranes in biotechnology are the following [2,3,4]: separation and harvesting of bacteria and enzymes, continuous high-performance bioreactors for enzymatic and microbial conversion processes, tissue culture reactor systems and whole-broth clarification.

Although Horst and Henemaaijer [1] concluded that adsorption did not play an important role in the fouling of microfiltration (MF) membranes, it seems that it may have an influence on some membrane processes. For example it is commonly recognized that adsorption modifies rejection properties of ultrafiltration (UF) membranes [5], especially for biopolymers which, while adsorbed, can change the effects of steric hindrance and hydration on membrane surface. The same may be true for MF membranes. Bowen and Hughes [6] have studied the influence of adsorption on flow rate and they found that even in the case of MF membranes there was a flux decline caused by adsorption. They also found a straightlinear relationship between the decrease of flow rate and adsorption. Another aspect of adsorption is when some valuable substances (e.g. vitamins, antibiotics) may be lost due to adsorption that affects the overall yield of the separation.

Adsorption on MF membranes has been relatively little studied, especially from the methodological point of view. It is well recognized that one of the main factors which has an influence on fouling and selectivity of UF membranes is adsorption at the initial stages of filtration [5-14] but up to now, only a few attempts have been made to study adsorption (for various types of membranes) in static [6,13,14] and dynamic [5,8,15-17] conditions. However, widely different results have been reported. Futhermore, three separate authors recently obtained varying results of BSA adsorption in terms of concentration isotherms at different pHs using different adsorbents and experimental protocols. Bowen and Hughes [6] obtained a broad maximum near the BSA isoelectric point, whereas Clark et al. [15] obtained a very sharp maximum around this point. Aluminium oxide (Al_2O_3) membranes of different types were used. The first group used MF membranes produced from anodized aluminium, and the second one Membralox membranes consisting of a thin gamma-aluminium layer on top of an alfa-aluminium support. A similar sharp peak around the isoelectric point was obtained by Donogh et al. [17] for polysulphone powder (used for membrane preparation) in static adsorption experiments. In earlier experiments related on adsorption of BSA on glass powder [18], the

existence of a broad maximum near BSA isoelectric point was found. Norde [19] found a similar trend for human serum albumin (HSA). It is difficult to draw any general conclusions based on these results. In turn, all the above results are contradictory to those obtained by Mathiasson [6], who using polymeric membranes, found a continuous decrease of adsorption as a function of pH (in the range pH 3.0-7.0) with the highest adsorption at pH 3.
In a previous paper [20], we presented a new quasi-dynamic method for measuring adsorption on tubular membranes, which was based on breakthrough curve determination. The main purpose of the present paper is the continuation of these studies for different pHs. For this reason, BSA was chosen as an adsorbate. Other arguments given by Bowen and Hughes [16], such as its availability in an highly purified form and extensive studies of its adsorption, were also important.
The method developed here in a good way simulates the conditions of an adsorption during UF or MF processes because adsorption takes place in the presence of permeation. Adsorption is caused by intermolecular forces, those which govern rejection mechanisms, especially for UF membranes.
The most important issue was to decide which of the previously presented methods (named by us algorithms [20]) used to determine the amount adsorbed on the membrane is the most suitable. Problem of pH's influence on BSA adsorption is a secondary one but anyway by this way we could obtain experimental results for a few systems using only one costly effective adsorbate (BSA).
An attempt has been made of modelling experimental adsorption isotherms in order to compare our results to those reported by several authors who used different methodologies. The present work corresponds to a beginning stage which presents the relevancy of using breakthrough curves for the investigation and characterization of MF membrane properties in relation to adsorption phenomena. Some comparisons of our results with those obtained by other authors may prove the validity of the method presented here. It also seemed of interest to discover whether the mechanism of protein adsorption on MF membranes is comparable to that of other adsorbents and whether filtration may induce changes in this mechanism.

MATERIALS AND METHODS

Materials

The water used during experiments was deionized, distilled and passed through the Millipore Q System. BSA (fraction V, 96-99% Albumin) was purchased from Sigma Chemical Company. The following BSA solutions used for adsorption experiments were : 0.125, 0.25, 0.5, 1 and 2 g/l; BSA solutions were prepared at four pHs: 3.0, 4.9, 7.4 and 9.5. For pH 3.0, 4.9 and 9.5, BSA was dissolved in 0.01 M NaCl solution and the pH was adjusted by the addition of small amounts of 0.1 M NaOH or HCl. For the solution preparation at pH 7.4, a Tris buffer was used (0.05 M Tris + 0.1 M HCl). The choice of such concentrations was based on the fact

that all absorbances could be measured in the same range of absorbance scale of the UV detector (1.28). For these concentrations the calibration curve, i.e. absorbance (in millivolt) vs. concentration, was straightlinear.
Two types of tubular membranes were used : Carbosep M14 (0.14 µm) and M20 (0.2 µm) microfiltration membranes (Tech-Sep, France) with an internal zirconium-titania oxide layer. Membrane is a monotube of 6 mm inner diameter, 10 mm external diameter and 1.2 m long. Each membrane of 1.2 m long was cut into pieces of 4.5 cm in length. After cutting, each piece was thoroughly washed by tap water and distilled water to remove dust and then boiled in distilled water for one hour and kept in distilled water for around 24 hours before using. Each membrane piece was used only once in adsorption measurements. The porous structure of M14 membrane and carbon support was characterized by mercury porosimetry (Micromeritics 9320 apparatus, Micromeritics, USA). The main characteristics of the porous structure are presented in Table 1. Pore size distribution (not presented here) exhibited two distinct peaks: one centred on 3 µm for carbon support, and another one centred on 0.14 µm corresponding to the M14 membrane cut-off. Specific surface area measured by mercury porosimetry for carbon support (2.26 m^2/g) is close to that expected for powdered carbon, i.e. 2 m^2/g. Specific surface area of M14 membrane is higher (of about twice as much) due to the upper separative layer mainly composed of zirconium oxide (specific surface area of commercial zirconium oxides is of the order of 40 m^2/g [42]).

Tab. 1. Physical properties of the membranes used as determined by mercury porosimetry.

Membrane type	Total pore area S (m^2/g)	Median pore diameter (volume) (µm)	Average pore diameter (4V/A) d_p (µm)	Porosity (vol/vol)
M14 (ZrO_2-C)	4.33	1.6	0.105	0.2
Carbon support	2.26	2.5	0.194	0.19

METHODS

Adsorption calculation from a breakthrough curve

BSA adsorption has been determined from the so-called breakthrough (BT) curve of typical S-shape profile. Such a curve is produced when a continuous stream of the solution passes through the adsorption column while continuous monitoring of the effluent concentration (or the outlet detector response).
The principle of the method is similar to column chromatography when portions of the effluent solution are collected by a fraction collector and then analyzed for concentration. In our method, time, effluent mass and detector response are acquired at equal time intervals. This interval can be chosen as one of the parameters of acquisition software. So for every time interval we observe a change in the effluent mass and a corresponding

detector response. It is exactly like having one portion of a solution in a fraction collector and a detector response corresponding to it. To calculate an adsorbed amount for such a virtual portion of the outlet solution, we have to estimate a difference in concentrations between this solution and inlet solution. By adding up adsorbed amounts for all virtual portions of the effluent solution along a BT curve, total adsorption on a given membrane for a given effluent mass is obtained. However, at this moment only, a problem exists of how to convert the detector response into adsorbed amounts.

On the basis of the general description of the method, this seems to be very simple, but an experimentation difficulty arises. It has usually been observed that this concentration (the detector response) is within the range of 0-10% less than that of the native one. Moreover, this part of the curve has some inclination, usually positive (but sometimes negative). To convert the detector response into the final adsorption, three methods (called by us algorithms [20]) were chosen and presented in Fig. 1. It is easy to show that if the detector response for inlet and outlet solutions after saturation of a BT curve was similar and constant, then all algorithms would give similar results irrespective of the effluent mass. The second problem is that for the determination of the amount of adsorbed BSA, it is also very important to establish a starting point on the breakthrough curve.

In the present study the approach proposed Walton and Koltisko was used [21]. From this approach, the starting point of integration corresponds to the point when BT curve starts to rise. The major change in the algorithms compared to those used in the previous paper [20] was that, for all of them, BT curve was always extrapolated (when needed) to a final experiment time of two hours. The point corresponding to this time was the last point of integration.

These three algorithms are as follows :

- for the first algorithm (Fig. 1a), the end of the continuous rising of the BT curve is found (point A). All data lying to the right of this point are added up and the arithmetic mean is calculated. This value is taken as the maximum absorbance. Shadowed area corresponds to calculated adsorption.
- for the second algorithm (Fig. 1b), point A is found as above and a regression line is fitted to all the data to the right of this point (using the least square method). Point B on the straight line is found that corresponds to a given effluent mass. Maximum absorbance is assumed to be equal to that of point B. Again shadowed area corresponds to calculated adsorption.
- for the third algorithm (Fig. 1c), the maximum absorbance is calculated from the calibration curve for a given concentration of the inlet solution.

Shadowed area is converted into the adsorbed amount using a trapezoidal method. This method is schematically presented in Fig. 1a. For a given narrow strip corresponding to a recorded effluent mass interval, an average absorbance is calculated and is converted into concentration using a calibration curve. The same is also made with maximal absorbance. This

difference in concentration multiplied by the difference in mass gives an adsorbed amount for a given strip (a black rectangle). By adding up all similarly calculated adsorbed amounts along the BT curve, total adsorption is obtained .

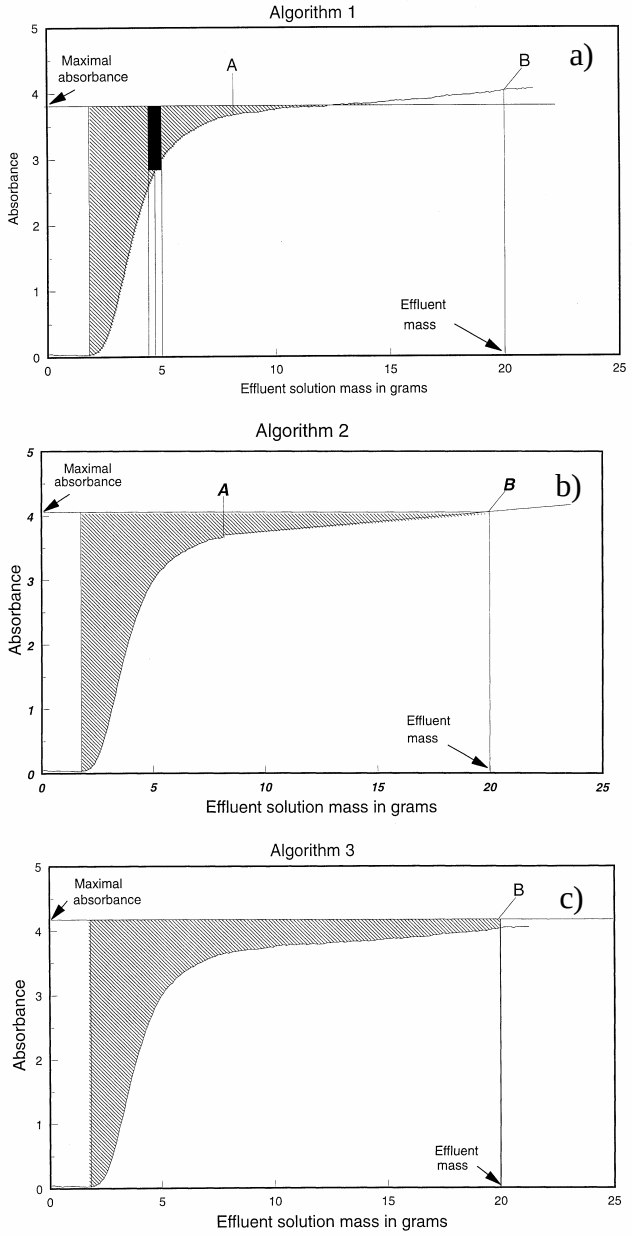

Fig. 1. Graphical presentation of algorithms studied for adsorption calculation. Fig. 1a: algorithm 1, Fig. 1b: algorithm 2 and Fig. 1c: algorithm 3.

Adsorption device

The device used for adsorption experiments is presented in Fig. 2. It consists of the following parts: 1) two thermostated modules with membranes, 2) two pumps for the solution and for the water, 3) an HPLC UV detector (Uvikon 730S LC, Kontron Ltd., Switzerland), 4) electrobalance (Mettler PM 4600), 5) two channels and a home-made data acquisition unit based on 6B modules (Analog Devices, USA) , 6) a PC microcomputer for data recording and handling, 7) an ultrathermostat (Haake F2, Germany), 8) a pressure storage tank for water to wash modules after experiments, 9) a pressure regulator, 10) an electronic pressure gauge and 11) two heat exchangers for water and solution to thermostate them before entering the membrane.

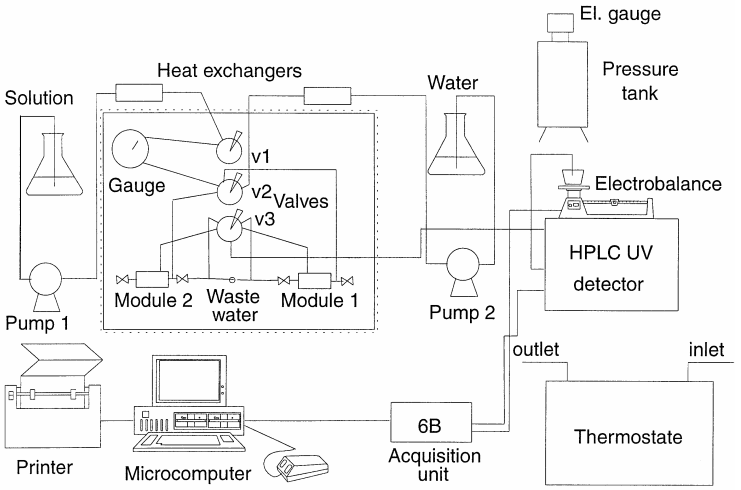

Fig. 2. Scheme of the device used for adsorption measurements.

Modules 1 and 2 are placed on a special manipulating board made of a PVC sheet along with three HPLC valves V1, V2 and V3 (Model 7000, Rheodyne, Inc., USA), and a gauge integrated with a pressure dampener for measuring pressure and reducing pulsations of the solution used. The valves are two position valves(three pairs of inlet-outlet sockets). Valve V1 is used for selecting a solution pump (it is possible to work with two solution pumps, but this option was not used in the experiments reported). Valve V2 is for switching the pumps from module to module. In one position pump 1 is connected to module 1, and pump 2 to module 2. In the second position the connection is reversed. Valve V3 is used to connect one module at a time to the detector. In the first position module 1 is connected to the detector and module 2 to the wastewater outlet. In the second position the

connection is reversed. Each module is fitted with two valves. One is to connnect the module to the wastewater outlet and the second is to quickly displace water by a solution from an internal volume of the membrane tube using a syringe.

Breakthrough curve determination

The measurement is performed by passing pure water through one of the membranes until minimal absorbance (i.e. very close to zero) is achieved. Pump 1 is switched on, valve V2 connects pump 1 and one of the modules, and the module outlet valve is opened for a few seconds. Then 10 ml of the solution is rapidly injected into the internal tube of the membrane to displace water by the solution, the outlet valve is closed, and data are recorded using the computer program. On the basis of recorded data, a BT curve, i.e., absorbance vs. weight, is constructed. During the experimentation the second membrane is washed by water. When the recorded curve showed only negligible changes in the absorbance, the experiment was stopped, the membrane was removed, and the module was washed by water from the pressure tank. Then the next membrane was placed into the module. When the membrane in the second module was ready to start, the above procedure was repeated for the second module.

Preparation of the calibration curve

Data for the preparation of the calibration curve were collected in the same session in which the adsorption experiments were carried out. Namely, after finishing the adsorption experiment, the membrane was removed and the solution studied was passed through the module and the detector. The computer program for data acquisition was run and acquisition of data was carried out for about 15 minutes. In fact, the detector response is not expressed in absorbance units but in millivolts, and this value was used to prepare the calibration curve. Then, a mean detector response was calculated. For BSA, a straightlinear correlation exists between the detector response (in millivolt) and concentration, and two regression coefficients are determined. These coefficients are input data for adsorption calculation using a computer program especially developed for this purpose. For every pH and concentration, adsorption was determined three times and the average value was taken for figure preparation and calculations.

RESULTS AND DISCUSSION

Influence of pH on BSA adsorption

In a previous paper [20], it was concluded that the method is particularly suitable to the study of adsorption of proteins on membranes. This problem was studied further and the results obtained are given in the present paper. Firstly, the effects of pH and BSA solution concentration at the same pump setting have been studied. Flow rate changed slightly between experiments and it was generally in the range 0.7 - 0.85 g/min.

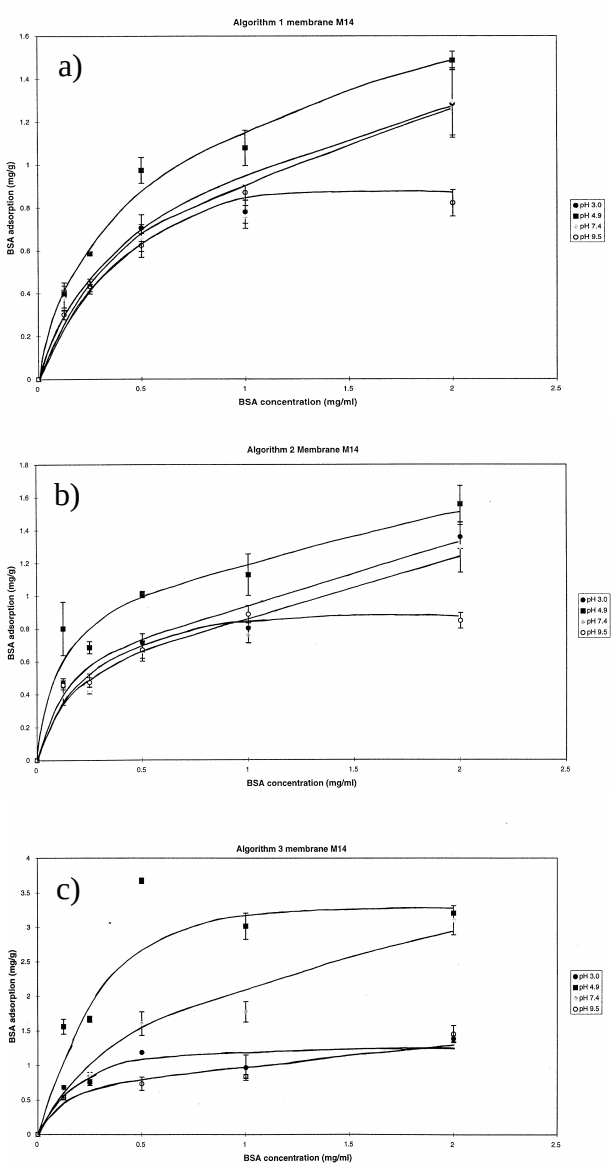

Fig. 3. Adsorption isotherms for BSA on M14 membranes at different pH's calculated according to: Fig. 3a: algorithm 1, Fig. 3b: algorithm 2 and Fig. 3c: algorithm 3, solid circles : pH 3.0, solid squares : pH 4.9, solid triangles : pH7.4, open circles : pH 9.5

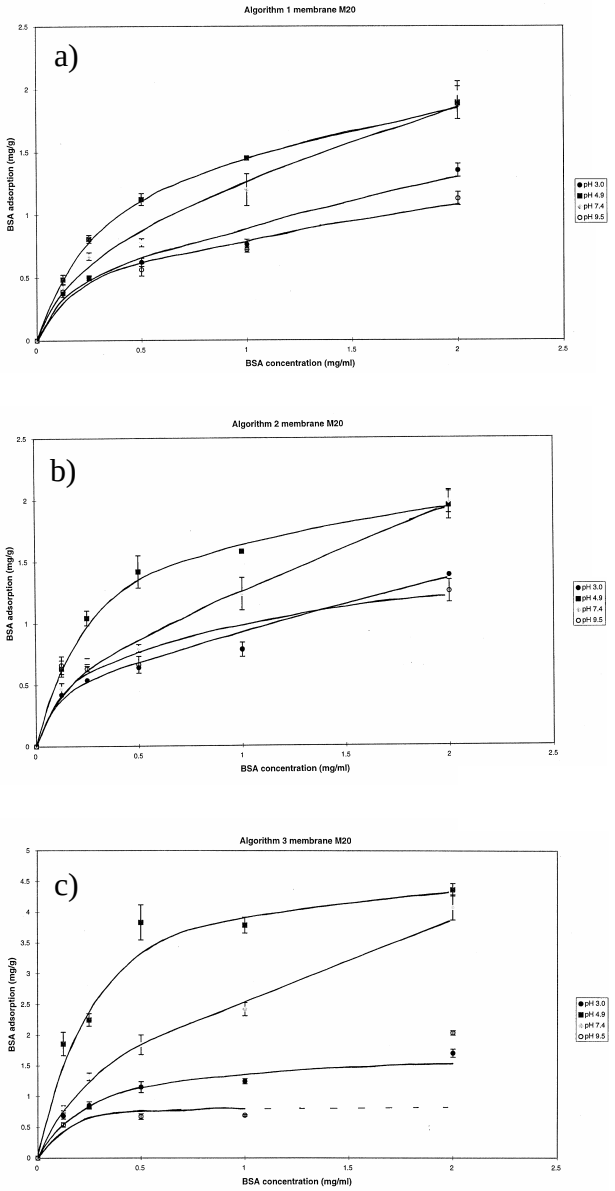

Fig. 4. Adsorption isotherms for BSA on M20 membranes at different pH's calculated according to: Fig. 4a: algorithm 1, Fig. 4b: algorithm 2 and Fig. 4c: algorithm 3, solid circles : pH 3.0, solid squares : pH 4.9, solid triangles : pH 7.4, open circles : pH 9.5

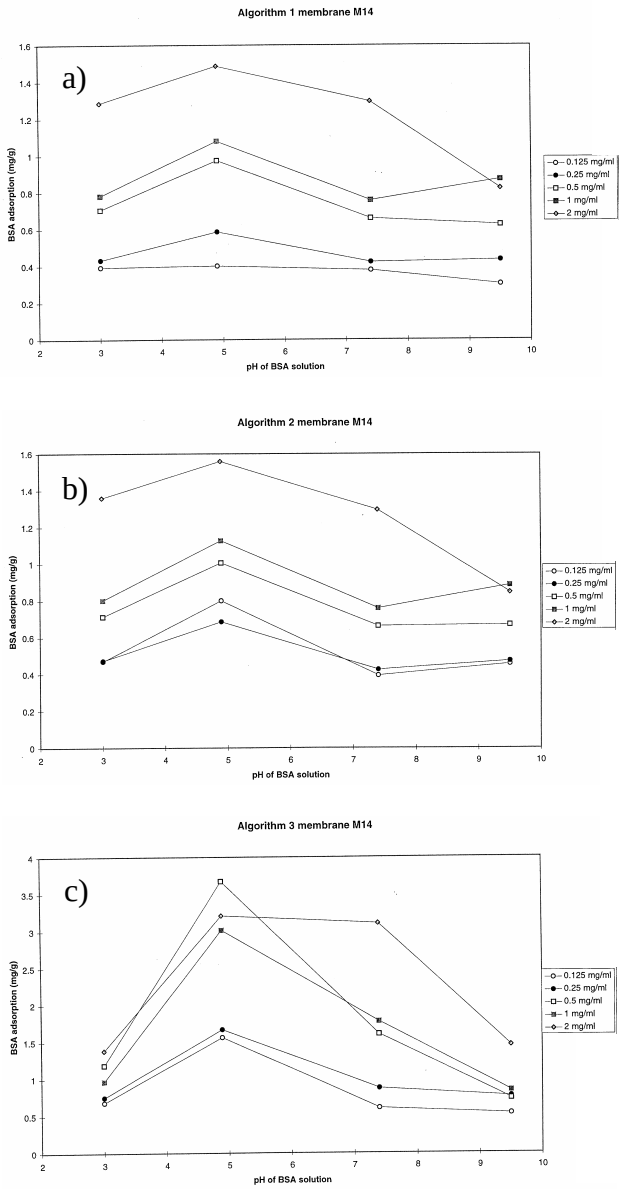

Fig. 5. Adsorption of BSA as a function of pH on M14 membranes at different concentrations calculated according to: Fig. 5a: algorithm 1, Fig. 5b: algorithm 2 and Fig. 5c algorithm 3, open circles : concentration 0.125 mg/ml, solid circles : concentration 0.25 mg/ml, open squares : concentration 0.5 mg/ml, solid squares : concentration 1 mg/ml, open triangles : concentration 2 mg/ml

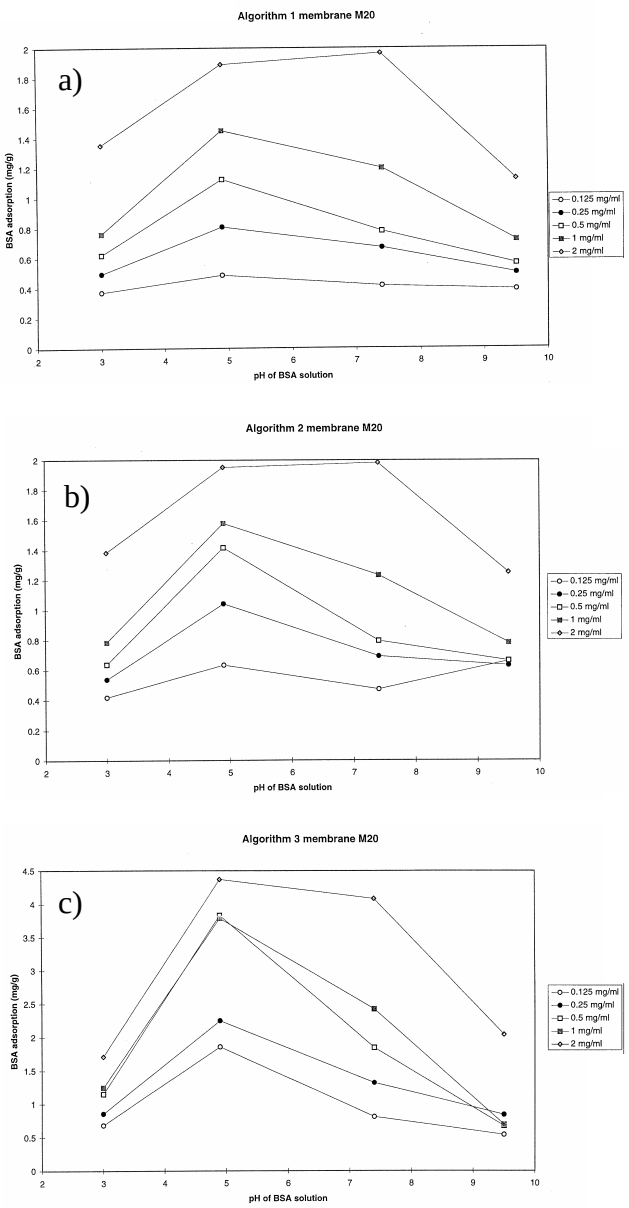

Fig. 6. Adsorption of BSA as a function of pH on M20 membranes at different concentrations calculated according to: Fig. 6a: algorithm 1, Fig. 6b: algorithm 2 and Fig. 6c: algorithm 3, open circles : concentration 0.125 mg/ml, solid circles : concentration 0.25 mg/ml, open squares : concentration 0.5 mg/ml, solid squares : concentration 1 mg/ml, open triangles : concentration 2 mg/ml

It was determined from the regression coefficient of straightlinear fitting to the recorded data for the effluent mass vs. time. Adsorption isotherms are plotted in Figures 3a, 3b and 3c (M14 membrane, algorithm 1, 2 and 3, respectively) and Figures 4a, 4b and 4c (M20 membrane, algorithm 1, 2 and 3, respectively). All marker points (i.e. circles, squares and triangles) correspond to an average adsorption value (usually on three experimental values) and marked error bars correspond to the standard deviation for the average value. When the error bar is not represented it means that its width is smaller than the marker point size.

Figs. 3 and 4 show that adsorption of BSA is influenced by concentration, algorithm used and pH. According to algorithms 1 and 2, adsorption isotherms do not have a well established plateau. Only algorithm 3 gives an adsorption isotherm with a plateau. Values given by algorithm 1 and 2 are similar but algorithm 3 gives much higher values of adsorption. Adsorption is higher on M20 membrane than on M14 one; pH influences the adsorption calculated according to all algorithms with the highest adsorption at pH 4.9. For a better understanding of this problem, adsorption as a of pH was at different concentrations in Figure 5 (5a, 5b and 5c) and Figure 6 (6a, 6b and 6c) for the same combination of membranes and algorithms as in Figs. 3 and 4. Figs. 5 and 6 clearly show that adsorption is the highest at pH 4.9, i.e. near the BSA isoelectric point, which has been already observed by many authors. The only exception are results for M20 membrane at 2 g/l concentration when, according to algorithms 1 and 2, adsorption is comparable for pH 4.9 and 7.4 (error bars overlap). Now we can try to decide which of the algorithms presented is correct. On the basis of the results obtained, it is evident that algorithms 1 and 2 give similar values of adsorption, whereas algorithm 3 gives much higher values. This problem will be discussed in detail later on.

Analysis of adsorption data variation

In general error bar widths are higher at the highest concentrations. However, in a few cases these widths are also higher for lower concentrations but this tendency has a random character. Standard deviation value is dependent on the average value (and thus on concentration). In order to compare the experimental error for all concentrations, another variable which is independent of concentration is more appropriate.

Therefore adsorption data variation has been studied through an analysis of the Variation Coefficient (noted VC) being the ratio of the sample standard deviation to the sample arithmetic mean (and usually expressed in percent). In Table 2 an analysis of VC is presented for all studied systems, i.e., for the different algorithms used for adsorption calculation, pHs, concentrations and membranes. Analysis has been performed for 40 systems (2 membranes x 4 pHs x 5 concentrations). This table consists of 8 columns. In the first one the algorithm is placed, in the second one the total number of systems studied, and next ones include: VC mean value for all systems studied,

number of systems for which VC is lower than 10%, number of systems for which VC is in the range 10-20%, number of systems for which VC is higher than 20%, minimal and maximal values of VC. For algorithm 1 the mean value of VC is 12.4% and varies from 1.3% to 30.9%. For 15 systems, VC is lower than 10%, for 4 ones it is higher than 20% and for 21 ones it is in the range 10-20%. For algorithms 2 and 3 similar data are presented in Table 2. Summarizing data listed in Table 2, it is seen that algorithm 3 gives the lowest mean value of VC and that for 20 systems VC is lower than 10%. It seems that the value of the maximum variation coefficient could be considered as being accidental since for every algorithm ,only one such high value appeared and the rest of VC values higher than 20% were essentially lower then 30%. It should be noted that no separate measurement has been rejected; sometimes rejecting one measured value could significantly improve VC.

Tab. 2. Variation coefficient (VC) for the systems studied.

Algo-rithm	Total number of systems studied	Mean value of VC (%)	Number of systems with VC < 10%	Number of systems with 0<VC<20%	Number of systems with VC > 20%	Min. value of VC (%)	Max. value of VC (%)
1	40	12.4	15	21	4	1.3	30.9
2	40	14.9	11	22	7	0.9	40.5
3	40	11.5	20	15	5	0.3	38.1

If we compare our adsorption data variation with the data of Robertson and Zydney [22], we can see that they obtained similar variations. They found that «data obtained from the same lot generally agreed to within ± 20%, with substantially larger variability (as much as a factor of two) obtained with membranes from different lots ». From the table 1 presented by them [22], it results that the variation coefficient ranged from about 9% to 30%. Variation coefficient for our results is thus comparable.

Analysis of the algorithms used for BSA adsorption calculation

Generally the influence of the algorithm used and pH is seen more clearly when adsorption is higher. Therefore differences in adsorption are lowest for M14 membrane and the algorithm 1. For this algorithm, adsorption values are mainly influenced by the first stage of adsorption when the main part of the BT curve is formed. Differences between algorithms 1 and 2 are slight since the difference is only in the upper limit of integration. For algorithm 3, the rise due to an increased upper limit of integration as well as to an increased area between maximal absorbance and BT curve, is quite appreciable. As Soderquist and Walton pointed out [23], in the first stage adsorption of proteins is spontaneous and quite random. Algorithms 1 and 2 probably reflect this stage. It is quite possible that

algorithm 3 includes the second stage of adsorption - structural change of adsorbed proteins. During calculations, it was found that algorithm 3 is very sensitive to even a small scatter of data used for calibration curve preparation. This is especially true for the highest concentrations. Therefore the method in question is better suited to linear calibration curves. For this reason, the method appears to be well suited for the study of adsorption in solutions of low protein content, generally less than 2 mg/ml (some aroma and colour compounds existing in such natural mixtures as beer, wine or fruit juices for example). In a previous paper [20] we found that algorithm 3 gave biggest scatter of data but this is not confirmed with the present study when VC for algorithm 3 is the lowest. So we can conclude that it has rather a random character related to the random non-homogeneity of membrane pieces. Therefore this algorithm should be recognized as the most correct and data scatter has a random character. If the method is considered as the equivalent to a fraction collector that automatically determines concentration in every fraction, this algorithm is the most logical.

Modelling of adsorption isotherms

Protein adsorption at solution-air and solid-solution interfaces has been studied by many authors. Some of these papers have reported a Langmuir-type adsorption isotherm at a solid-solution interface [8,9,22], despite the fact that none of the Langmuir premises (like reversibility, adsorption on fixed sites, lateral interactions) are satisfied.

As far as an adsorption of proteins on a microporous membrane surface is concerned, literature data are much more scarce. The problem is, however, whether a mechanism of adsorption is similar for typical adsorbents. During filtration of a solution through a membrane, such phenomena as mass transfer limitation, sieving effect or solute build-up at the membrane surface can be misinterpreted as an equilibrium adsorption. Of course, by studying only changes of the solution concentration during filtration, it would be difficult to find a complete solution of this problem. We believe, however, that a thorough analysis of the shape of adsorption isotherms and of the monolayer capacity could provide some valuable information on these effects. Adsorption of solutes flowing through the membrane has been found to occur in many cases in micro- and ultra-filtration, especially when biological solutions are treated. It is essential to know how adsorption may influence and enhance membrane fouling in membrane separation processes. According to Norde [19], a multilayer protein adsorption seems improbable because desorption hardly ever occurs. Multilayer adsorption is improbable even in the case of "kinked" isotherm with two plateaux [19]. He accepts the explanation of Fair and Jamieson [24] who proposed a mechanism of bimodal adsorption of proteins. At low protein concentration the molecules adsorb in a random independent way, and in this region the isotherm is similar to the Langmuir one; then, after reaching a short plateau, there is S-shaped transition region corresponding to a more or less

unordered, glassy structure, followed by third region of formation of a two-dimensional protein crystal. At this moment the isotherm reaches the second plateau. This type of adsorption isotherm has been obtained by several authors with different proteins, adsorbents and concentration ranges [22,24,25]. This adsorption mechanism is potentially useful in explaining membrane fouling by proteins.

Our isotherms fit approximately the first second regions. shape suggests an analysis in terms of the Langmuir equation. Substrata of membranes are rather non-homogeneous as to their adsorption abilities, which is manifested by a wide scatter of adsorption data for different pieces of the same membrane. This may be caused by the non-homogenous pore structure of membranes. Nevertheless it seems interesting to investigate an adsorption mechanism for MF membranes at low BSA concentrations. In practice, during beer crossflow microfiltration [26], mixtures of such low soluble protein content are encountered. Therefore it would be interesting to know if soluble protein can act as a foulant at such low concentrations. Comparisons of the calculated monolayer capacity may provide information about whether the mechanism of adsorption for MF membranes is similar to that for other adsorbents, and whether the above mentioned effects can give rise to BSA uptake by a membrane. For this reason one model was used to determine the monolayer capacity of the membrane studied. Determination of the monolayer capacity has the advantage of taking an isotherm plateau value as an example, being based on all adsorption points and not on a single one giving a more precise result. If we compare the mean pore diameter of the membranes used (0.14 µm for M14 and 0.2 µm for M20) with the biggest size of BSA molecule (14 nm along the longest axis of the molecule [22]), it is evident that pore diameter is about ten or so times higher, as determined by mercury porosimetry (Table 1). Steric retention would not be thus expected to be significant as it will be shown further.

Langmuir's model

This isotherm can be written in its linearized form as:

$$\frac{1}{a} = \frac{1}{K\, a_{\mathrm{m}}\, c} + \frac{1}{a_{\mathrm{m}}} \qquad (1)$$

where a is adsorbed amount, c is concentration, a_{m} is Langmuir monolayer capacity and K is a binding constant The value of a_{m} corresponds to the plateau value of this isotherm. Two constants a_{m} and K can be determined by a least square fitting of data $1/a$ vs. $1/c$.

Using adsorption data presented in Figs. 3 and 4, both constants have been determined. In Fig. 7 Langmuir monolayer capacity a_{m} (in mg/g) is plotted as a function of pH for M14 and M20 membranes for the three algorithms studied. Fig. 7 shows that this capacity is dependent on membrane type, algorithm used and pH. However the difference between the algorithms 1 and 2 is negligible; a_{m} is influenced by pH giving the highest capacity at pH

4.9, i.e. BSA isoelectric point. It is also clear that M20 membrane adsorbs more M14 membrane M14.

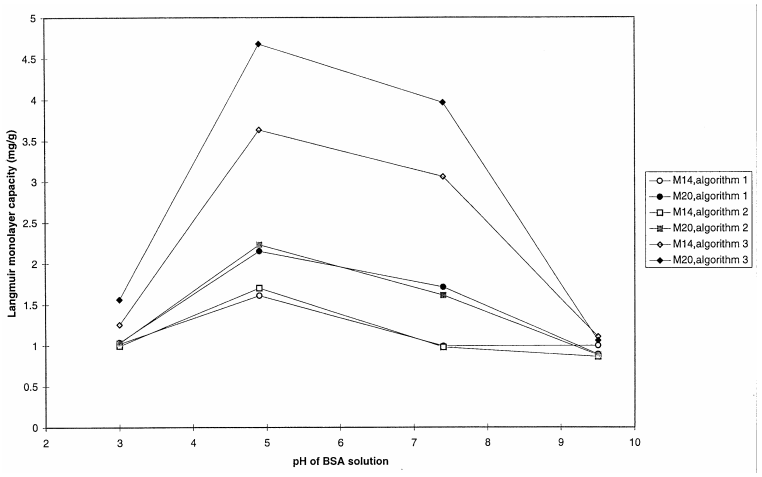

Fig. 7. Langmuir monolayer capacity a_m as a function of pH, open circles,squares and triangles : M14 membranes, solid circles,squares and triangles : M20 membranes, algorithm 1 : circles, algorithm 2 : squares, algorithm 3 : triangles

Linear correlation of data 1/*a* vs. 1/*c* means that the Langmuir equation is fulfilled. Statistics provides methods which can indicate whether a given correlation is significant or not. We have made such attempts, and the results are presented below. The Student's *t*-test [27] was used to find which correlation coefficients of the twenty four systems (3 algorithms x 2 membranes × 4 pHs) were significant. A tested null hyphothesis was that the correlations presented were not significant and were only caused by random errors. Results of this analysis are presented in Table 3.
The table includes the following columns: pH, square of a correlation coefficient, correlation coefficient and value of t_{cal}. If t_{cal} is bigger than the t value, then we cannot accept the null hypothesis that the correlation is not significant. In the next three columns corresponding to four different significance levels, significant correlations are marked by asterix and not significant ones by n. It can be seen that for M14 membranes, only one correlation is not significant and for M20 ones two. For the rest of fittings, correlations were significant at a significance level of 0.05 or in many times even at 0.001.

Tab. 3[a]. Statistical analysis of the correlation between adsorption calculated from Langmuir equation and adsorption measured for the systems studied.

Algorithm	pH	Square of correlation coefficient	Correlation coefficient	t_{cal}	0.1[b] 2.131[c]	0.05[b] 2.776[c]	0.01[b] 4.604[c]	0.001[b] 8.61[c]
M14 membranes								
1	3.0	0.842	0918.	4.617			*	
1	4.9	0.985	0.992	16.207				*
1	7.4	0.845	0.919	4.670			*	
1	9.5	0.986	0.993	16.784				*
2	3.0	0.739	0.860	3.365		*		
2	4.9	0.528	0.727	2.115	n			
2	7.4	0.817	0.904	4.226		*		
2	9.5	0.812	0.901	4.157		*		
3	3.0	0.784	0.885	3.810		*		
3	4.9	0.775	0.880	3.712		*		
3	7.4	0.969	0.984	11.182				*
3	9.5	0.783	0.885	3.799		*		
M20 membranes								
1	3.0	0.908	0.953	6.283				*
1	4.9	0.998	0.999	44.677				*
1	7.4	0.956	0.978	9.323				*
1	9.5	0.871	0.933	5.197			*	
2	3.0	0.869	0.932	5.151			*	
2	4.9	0.993	0.997	23.821				*
2	7.4	0.928	0.963	7.180			*	
2	9.5	0.380	0.616	1.566	n			
3	3.0	0.945	0.972	8.290			*	
3	4.9	0.927	0.963	7.127			*	
3	7.4	0.986	0.993	16.784				*
3	9.5	0.460	0.678	1.846	n			

[a]Degrees of freedom : $i = 4$.
[b]Significance level
[c]Student's t test for $i = 4$.
n : correlation was not significant

Determination of the specific surface area of M14 membrane

Giles [28,29] found that from an adsorption of p-nitrophenol (PNP) from water or aromatic hydrocarbons, it is possible to determine specific surface area on non-porous solids. This solute gives values similar to those obtained by nitrogen adsorption.

In a previous work [20] we determined static adsorption of phenol on M14 membrane. Giles [29] assumed close packing and flatwise orientation of PNP molecule in a monolayer, occupying 52.5 ? ^{2}. We assume that the area occupied by the phenol molecule is similar to that for PNP and is connected to the size of the benzene ring. For example the area for benzene molecule is 43.6 ? ^{2} and for toluene molecule 55.2 ? ^{2} [30]. Therefore 52.5 ? ^{2} appears to be a reasonable value for phenol. Using data of phenol static adsorption

and Langmuir equation (viz. eqn. 1), its monolayer capacity was determined. Calculated value was 10.5 micromole/g. Using those data, calculated specific surface area for M14 membrane was 3.32 m^2/g. This value seems to be reasonable and is in a fairly good agreement with that measured by mercury porosimetry (i.e. 4.33 m^2/g).

Estimation of BSA monolayer capacity on M14 membranes

In Table 4 are listed monolayer capacities (in mg/m^2) for M14 membrane calculated from the Langmuir equation for the three algorithms studied using calculated above specific surface area. These capacities were calculated by dividing Langmuir monolayer capacity in mg/g by specific surface area in m^2/g. If we compare data in Table 4, we can only confirm previously drawn conclusions, namely, that algorithms 1 and 2 give very similar values and algorithm 3 gives higher values. The higher the adsorption, the higher the difference between the third, and first and second algorithms. Quoted theoretical BSA monolayer capacity in side-on orientation is 2.5 mg/m^2 [22], and similar values are reported for many adsorbents [19]. From this point of view data for the third algorithm at pH 4.9 and 7.4 seem to be quite reasonable. It may also be concluded that an experimental time of two hours is not sufficient to achieve the full monolayer or that BSA concentration is too low to reach a plateau value.

Tab. 4. BSA monolayer capacities (in mg/m^2) for M14 membrane calculated from the Langmuir isotherm.

pH	BSA monolayer capacity (mg/m²)		
	Algorithm 1	Algorithm 2	Algorithm 3
3.0	0.31	0.30	0.38
4.9	0.49	0.51	1.09
7.4	0.30	0.30	0.92
9.5	0.30	0.26	0.33

This would explain the observed BT curve gradient, corresponding to a continuous build-up of a monolayer. Another explanation may be provided by Weinbrenner and Etzel [31] who, studying adsorption of BSA on a sulfopropyl ion-exchange membrane, found that competetive adsorption caused displacement of bound BSA monomer by a more strongly binding BSA dimer. They determined BT curves for BSA adsorbed to the sulfopropyl MemSep 1010 ion-exchange membrane chromatography cartridge contained in a stack of 72 regenerated cellulose membranes of 1.2 µm pore size. They found that after an effluent volume of 350 ml, the effluent concentration of BSA rose to only 96% of the feed solution concentration; BSA dimer concentration in the effluent continued to rise slowly but did not reach the concentration dimer in the feed solution. They

also cited a paper of Skidmore et al. [32] who found that BT curves of BSA for a sulfopropyl gel-bead packed column did not reach the feed solution concentration either. Their explanation was that the slow formation of dimers on the surface resulted in the removal of the monomer from solution leading to the lowering of monomer concentration in the effluent.

Effect of steric retention and fouling on adsorption calculation with M14 membranes

As mentioned above, the convective transport of a solute inside the membrane is likely to cause fouling (essentially protein deposition induced by flow through the pores) responsible for the rejection of the solute from the membrane (via steric hindrance or concentration polarisation for instance). Such a fouling-induced retention, superimposed upon adsorptive retention, can be misinterpreted as a equilibrium adsorption and lead to an error or scatter in the estimation of the adsorbed amount. As shown in Table 4, the calculated BSA monolayer capacity is significantly lower (of about 75%) than the theoretical one (2.5 mg/m^2). Moreover it has been observed that for most of the runs, maximum absorbance of BT curves (as illustrated in Fig. 1c) was lower than inlet solution absorbance (up to 10%, corresponding to A_{max}=0.9A_{inlet}). As it can be seen in Table 4, BSA monolayer capacity is the highest for algorithm 3 which corresponds to the case where adsorption, in the absence of any sieving effects, is the sole solution transport process. The observation of a maximal absorbance inferior to inlet solution absorbance after an experimental time of two hours seems to indicate that, due to transport limitations, some depletion of BSA concentration in the effluent actually occurred. Since the diameter of a BSA molecule is well lower than that of a membrane pore (with a size ratio of the order of 1/20), concentration polarisation over the membrane surface is unlikely, so that only the steric retention of BSA molecules has been considered in evaluating the effect of transport limitations on adsorption calculation. We have considered the simple and convenient case of steric retention (according to Ferry [33]) of a solute of radius r_s by a pore whose radius r_p is decreased in value by the thickness of a monolayer adsorbed, as reported by Zeman [34]. Steric retention is described as follows :

$$R=1-C_p/C_0 = [\lambda'(\lambda'-2)]^2 \qquad (2)$$

where C_p is the concentration of solute in permeate (or effluent concentration), C_0 the concentration of solute in retentate (or inlet solution concentration) and λ' the ratio of solute radius to effective pore radius. In the case of an adsorbing solute, λ' is given by :

$$\lambda' = r_s/(r_p-\delta) \qquad (3)$$

where δ is the adsorbed layer thickness. The effective thickness of the adsorbed layer on pore wall is found from :

$$\delta = m/(\rho_s S) \quad (4)$$

where m is the adsorbed solute mass at equilibrium adsorption given by Langmuir monolayer capacity, *S* the total surface area of the membrane and ρ_s specific mass of solute; *m/S* represents the mass of adsorbed solute per unit total surface area of membrane, i.e. the monolayer capacity in mg/m?. The porosity of the protein layer adsorbed on the inner pore walls is assumed to be negligible. BSA molecule radius (r_s) was considered as equal to 3.5 nm [35] and pore radius (r_p) was set as equal to the average pore size measured by mercury porosimetry, i.e. 53 nm (see Table 1). Using BSA monolayer capacities determined in Table 4 and assuming BSA has a specific mass of 1.0 g/cm^3, steric retention R derived from eqns. (2), (3) and (4) for the various algorithms and pHs is presented in Table 5. Table 5 shows that the predicted adsorbed layer thickness onto the pore wall ranges from 0.3 to 1 nm, which leads to a corresponding pore section decrease from 1 to 4 %. Predicted steric retention varies very little under the conditions used with the majority of values close to 1.7 %; also this retention level was found to be very close to that of the clean membrane (1.6 %), in agreement with the expected insignificant enhancement of steric retention due to the build-up of a BSA monolayer. Calculated adsorbed layer thicknesse δ is significantly lower than the molecular size of BSA ($4.2 \times 4.2 \times 14.1$ nm [36]), giving only a sub-monolayer or an incomplete protein coverage, as suggested by the slight and continuous increase in the adsorbed amount with solution concentration shown in Figures 3 and 4. The low variation of R with δ can be related to the characteristic profile of the sigmoidal steric rejection curve [34] (i.e. R versus λ), which is quite constant and insensitive to λ at low values of λ; also it must be noted that calculated values of λ (close to 0.07) lie in the lower part of the validity range of Ferry's equation ($0.2 < \lambda < 0.8$) making retention values calculated in Table 4 approximate.

Tab. 5. Steric retention R (eqn. 2) and relative pressure drop increase $\Delta P/\Delta P_0$ (eqn. 5) due to fouling for the various algorithms and pHs used.

pH	Algorithm 1			Algorithm 2			Algorithm 3		
	δ* (nm)	R (%)	$\Delta P/\Delta P_0$ ( )	δ (nm)	R (%)	$\Delta P/\Delta P_0$ ( )	δ (nm)	R (%)	$\Delta P/\Delta P_0$ ( )
3	0.31	1.65	1.024	0.3	1.65	1.023	0.38	1.65	1.029
4.9	0.49	1.66	1.038	0.51	1.66	1.039	1.09	1.7	1.087
7.4	0.3	1.65	1.023	0.3	1.65	1.023	0.92	1.687	1.072
9.5	0.3	1.65	1.023	0.26	1.65	1.02	0.33	1.65	1.025

* Adsorbed layer thickness derived from the values of BSA monolayer capacity (mg/m²) in Table 4.

DISCUSSION

If one assumes a constant steric retention of 1.7 % throughout a BT curve run with an absorbance proportional to solution concentration, it may be calculated that maximal absorbance in the effluent would be equal to 0.98 times the absorbance of the inlet solution (i.e. $A_{max}=0.98A_{inlet}$). Hence, steric retention can be considered as being negligible as a mass transfer limitation. The lowering of maximal absorbance observed experimentally (~10 %, i.e. $A_{max}=0.9A_{inlet}$) is then thought to arise from other transport mechanisms. For example recent studies of Kelly and Zydney [37,38] clearly showed the decisive role played by protein aggregates in membrane fouling. In addition, as the adsorbed amount was found to be sensitive to maximal absorbance (especially for algorithm 3), it is likely that the predicted slight depletion of effluent concentration due to steric retention (R=1.7%), possibly strengthened by pore blocking, deposition of aggregates inside the membrane or slow formation of dimers, tends to reduce the maximal effluent absorbance.

At this stage, a question arises about the actual definition of adsorption on MF membranes and about the relevancy of using BT curves to quantify it. In particular an important point is the distinction between protein *adsorption* and protein *deposition* (fouling), as was pointed out by some authors [39,40]. Strictly speaking, adsorption is a thermodynamically spontaneous process which implies an equilibrium process with partitioning of solute between a solution and a surface [39]; under permeation conditions, adsorption will play a role but there will be an additional influence of convection-induced deposition (essentially a protein-protein interaction induced by shear flow in membrane pores). Adsorption within the membrane determined here is believed to reflect the first step in the fouling process encountered in UF and MF (and usually a precursor to long term flux decline). BSA adsorption quantified in this work may be related to the internal and strongly-bound protein fouling which has been observed both through partially permeable UF membranes [5,41] and MF membranes [26,42]; characteristic profiles of flux and rejection versus time were then produced, which are believed to be a manifestation of early protein adsorption into membrane pores leading to a depletion of protein in permeate similar to that exhibited by BT curves.

The detrimental effect of an adsorbed layer on membrane permeability may be assessed using the Poiseuille equation. At constant flow rate, the relative transmembrane pressure increase (or corresponding flux decrease at constant pressure filtration) can be written as :

$$\Delta P/\Delta P_0=[1-(\delta/r_p)]^{-4} \qquad (5)$$

where ΔP_0 is pressure drop across the reference clean membrane. It is seen in Table 5 that, under the various conditions used, relative transmembrane

pressure increase $\Delta P/\Delta P_0$ (or membrane permeability decrease) due to an adsorption related pore constriction ranges from 2 to 8 %. This result conforms to the small increase (of about 10 %) of entry pressure that has been observed during BT curve runs with BSA solutions on M14 membranes. Adsorption is thus intimately linked to the permeation and retention properties of MF membranes for an adsorbing solute. The amount of BSA adsorbed (of the order of a monolayer) resulted in a negligible loss of membrane permeability, but also in a significant one of protein in the effluent (permeate) until a full monolayer is formed. The latter phenomenon will be all the more pronounced as the specific surface area of the membrane is high.

An interesting feature may be provided by the comparison of the operating conditions used in adsorption measurement through BT curves with those that typically prevail in CFMF processes. Considering a constant flow rate in the range 0.7-0.85 ml/min and a membrane resistance of 10^{12} m^{-1} for M14 membrane, we calculate that it would be comparable to a crossflow filtration run with a permeate flux of 50 l/h.m? and a transmembrane pressure of 0.1 bar. Such permeation conditions can reasonably be considered as representative of those existing in the long term flux decline phase for the CFMF of biological feeds containing proteins (e.g. fermentation broths). In addition it is noted that, unlike most of adsorption studies on UF/MF membranes which generally refer to the filter membrane surface area in the estimation of the amount adsorbed, we have considered here the total surface area of the membrane, i.e. the external plus internal membrane area. Calculation of the amount of BSA adsorbed per unit filter surface area (0.00085 m? for a membrane of 4.5 cm long) gives values between 450 and 1500 $\mu g/cm^2$; such values are considerable and are of the same order of magnitude that some reported values for protein adsorption on UF [5,9,12,14,43,44] and MF [16,26] membranes either in static or dynamic conditions.

To sum up this paragraph, we can state that such phenomena as pore blocking, deposition of aggregates or slow formation of dimers may reduce the maximal effluent absorbance, but they have a minor effect on BT curve shape. Therefore we can conclude that BT curves determined for inorganic MF membranes are governed by pure adsorption and diffusion. Only the 'tail' of the BT curve may be influenced by the above mentioned phenomena, as determined from the calculations considering an ideal steric rejection as a first approximation. It seems that the main factor responsible for such a behaviour is the relative low BSA concentration used in comparison with that encountered in biological feeds processed by CFMF (e.g. beer, whey). At higher concentrations, the detrimental effect on adsorption calculation of the above mentioned phenomena would have been probably higher.

CONCLUSIONS

Based on the data presented in this paper, the following set of conclusions may be drawn:

1. The previous conclusion [20] that the developed method is suitable for protein adsorption has been fully confirmed.
2. It seems that the most reasonable results are provided by algorithm 3, for which maximal absorbance of the effluent is equal to inlet solution absorbance.
3. Adsorption of BSA was found to be sensitive to pH, and its maximum is near BSA isoelectric point, as reported by many authors on other adsorbents using various methods for its determination.
4. Adsorption determined for the highest studied concentration (2g/l) is comparable or even lower than the monolayer capacity, which proves that for this high concentration, adsorption is of monomolecular type or even less.
5. Monolayer capacities found are not in contradiction with those obtained for other solid/BSA solution systems as well as for BSA solution/air systems.
6. It seems that the mechanism of adsorption on mineral MF membranes is not particularly different to that of adsorbents in powdered form.

Based on this, we can conclude that such effects as pore blocking, deposition of aggregates inside the membrane or slow formation of dimers are not the main mechanisms of BSA uptake for the studied MF membranes.

Acknowledgements

The authors wish to than Tech_Sep Company for providing the membranes and Mr. P. Paulier (Universite Technologique de Compiegne, France) for mercury porosimetry measurements.

List of symbols

a	adsorbed amount (mg/g)
A	absorbance at 280 nm ()
a_m	Langmuir monolayer capacity (mg/g)
c	solution concentration (mg/ml)
C_p	effluent (or permeate) concentration (kg/m^3)
C_0	inlet (or retentate) concentration (kg/m^3)
K	binding constant, eqn. 1 (ml/mg)
m	mass of adsorbed solute (kg)
ΔP	pressure drop across the membrane (Pa)
R	steric retention, eqn. 2 ()
r_p	average pore radius of the membrane (nm)
r_s	solute radius (nm)
S	total surface area of the membrane (m²)

Greek letters

δ	adsorbed layer thickness (nm)
λ'	ratio of solute radius to effective pore radius, eqn. 3 ()
ρ_s	specific mass of solute (g/cm^3)

REFERENCES

[1] H.C. Van der Horst and J.H. Hanemaaijer, Cross-flow microfiltration in the food industry. State of the art, *Desalination* 1990, *77*, 235-258.

[2] U. Merin and G. Daufin, Separation processes using inorganic membranes in the food industry , Proceeding of the First International Conference on Inorganic Membranes (ICIM), Montpellier (France), July 3-6, J. Charpin and L. Cot Eds., 1989, 271-281.

[3] G. Cueille and M. Ferreira, Place of mineral membranes in the processes for bio-industry and the food industry, Proceeding of the First International Conference on Inorganic (ICIM) Membranes, Montpellier (France), July 3-6, J. Charpin and L. Cot Eds., 1989, 303-310.

[4] A.S. Michaels and S.L. Matson, Membranes in biotechnology: State of the art, *Desalination* 1985, *53*, 231-258.

[5] A.G. Fane, C.J.D. Fell and A.G. Waters, Ultrafiltration of protein solutions through partially permeable membranes. The effect of adsorption and solute environment, *J. Membrane Sci.* 1983, *16*, 211-224.

[6] W.R. Bowen and D.T. Hughes, Properties of microfiltration membranes. Part 2. Adsorption of bovine serum albumin at aluminium oxide membranes, *J. Membrane Sci.* 1990, *51*, 189-200.

[7] E. Matthiasson, The role of macromolecular adsorption in fouling of ultrafiltration membranes, *J. Membrane Sci.* 1983, *16*, 23-36.

[8] W.J. Dillman and J.F. Miller, On the adsorption of serum proteins on polymer membrane surfaces, *J. Colloid Int. Sci.* 1973, 44, 221-241.

[9] K.C. Ingham, T.F. Busby, Y. Sahlestrom and F. Castino, Separation of macromolecules by ultrafiltration: influence of protein adsorption, protein-protein interactions and concentration polarization, In Polymer Science and Technology, Ultrafiltration Membranes and Application; A.R. Cooper Eds., Plenum,New York, Vol. 13, 1981, 141-158.

[10] E. Matthiasson, B. Hallstrom and B. Sivik, In Engineering and Food, B. McKenna Eds., Elsevier Applied Science Publishers, New York, Vol. 1, 1984, 139-149.

[11] H. Nabetani, M. Nakaima, A. Watanabe, S. Nakao and S. Kimura, Effect of osmotic pressure and adsorption on ultrafiltration of ovalbumin, *AIChE Journal* 1990, *36*, 907-915.

[12] A. Suki, A.G. Fane and C.J.D. Fell, Flux decline in protein ultrafiltration, *J. Membrane Sci.* 1984, *21*, 269-283.

[13] L.E.S. Brink and D.J. Romijn, Reducing the protein fouling of polysulfone surfaces and polysulfone ultrafiltration membranes: Optimization of the type of presorbed layer, *Desalination* 1990, *78*, 209-233.

[14] P. Aimar, S. Baklouti and V. Sanchez, Membrane-solute interactions : Influence on pure solvent transfer during ultrafiltration, *J. Membrane Sci.* 1986, *29*, 207-224.

[15] W.M. Clark, A. Bansal, M. Sontakke and Y.H. Ma, Protein adsorption and fouling in ceramic ultrafiltration membranes, *J. Membrane Sci.*, 55 (1991) 21-38

[16] W.R. Bowen and D.T. Hughes, Properties of microfiltration membranes.Part 1. Adsorption of trypsin inhibitor at aluminium oxide membranes, Proceeding of the First International Conference on Inorganic Membranes (ICIM), Montpellier (France), July 3-6, J. Charpin and L. Cot Eds., 1989, 147-152.

[17] R.M. McDonogh, H. Bauser, N. Stroh and H. Chmiel, Concentration polarization and adsorption effects in cross-flow ultrafiltration of proteins, *Desalination* 1990, *79*, 217-231.

[18] H.B. Bull, Adsorption of bovine serum albumin on glass, *Biochim. Biophys. Acta* 1956, *19*, 464-471.

[19] W. Norde, Adsorption of proteins from solution at the solid-liquid interface, *Adv. Colloid Int. Sci.* 1986, *25*, 267-340.

[20] T. Bialopiotrowicz and M.N. Leclercq-Perlat, Studies on dynamic adsorption on inorganic membranes, *Langmuir* 1993, 9(10), 2703-2711.

[21] A.G. Walton and B. Koltisko, Protein structure and the kinetics of interaction with surfaces, *Adv. Chem. Ser.* 1982, *199*, 245-260.
[22] B.C. Robertson and A.L. Zydney, Protein adsorption in asymmetric ultrafiltration membranes with highly constricted pores, *J. Colloid Int. Sci.* 1990, *134*, 563-575.
[23] M.E. Soderquist and A.G. Walton, Structural changes in proteins adsorbed on polymer surfaces, *J. Colloid Int. Sci.* 1980, *75*, 386-396.
[24] B.D. Fair and A.M. Jamieson, Studies on protein adsorption on polystyrene latex surfaces, *J. Colloid Int. Sci.* 1980, *77*, 525.
[25] E. Kiss, Temperature dependence of bovine serum albumin adsorption onto poly(ethylene oxide)-grafted surface, *Colloids Surfaces A: Phys. Eng. Aspects* 1993, *76*, 135-140.
[26] P. Blanpain, J. Hermia and M. Lenoel, Mechanisms governing permeate flux and protein rejection in the microfiltration of beer with a Cyclopore membrane, *J. Membrane. Sci.* 1993, *84*, 37-51.
[27] J. Czerminski, A. Iwasiewicz, Z. Paszek and A. Sikorski, Statistical methods in applied chemistry, PWN-Polish Scientific Publishers, Warsaw, Elsevier-Amsterdam-Oxford-New York, 1990.
[28] C.H. Giles, I.A. Easton, R.B. McKay, C.C. Patel, N.B. Shah and D. Smith, Association of adsorbed aromatic solutes, *Trans. Faraday Soc.* 1966, *62*, 1963-1975.
[29] C.H. Giles and A.P. D'Silva, Molecular sieve effects of powders towards dyes. Measurement of porosity by dye adsorption, *Trans. Faraday Soc.* 1969, *65*, 1943-1951.
[30] A.L. McClellan and H.F. Harnsberger, Cross-sectional areas of molecules adsorbed on solid surfaces, *J. Coll. Int. Sci.* 1967, *23*, 577-599.
[31] W.F. Weinbrenner and M.R. Etzel, Competitive adsorption of α-lactalbumin and bovine serum albumin to a sulfopropyl ion-exchange membrane, *J. Chromatography (Part A)* 1994, *662*, 414-419.
[32] G.L. Skidmore, B.J. Horstman and H.A. Chase, Modelling single-component protein adsorption to the cation exchanger S Sepharose® FF, *J. Chromatography* 1990, *498*, 113-128.
[33] J.D. Ferry, Statistical evaluation of sieve constants in ultrafiltration, *J. Gen. Physiology* 1936, *20*.
[34] L.J. Zeman, Adsorption effects in rejection of macromolecules by ultrafiltration membranes, *J. Membrane Sci.* 1983, *15*, 213-230.
[35] M.W. Chudacek and A.G. Fane, The dynamics of polarisation in unstirred and stirred ultrafiltration, *J. Membrane Sci.* 1984, *21*, 145-160.
[36] T. Peters, Serum Albumin, *Adv. Protein Chem.* 1985, *37*, 161-245.
[37] S.T. Kelly, W.S. Opong and A.L. Zydney, The influence of protein aggregates on the fouling of microfiltration membranes during stirred cell filtration, *J. Membrane Sci.* 1993, *80*, 175-187.
[38] S.T. Kelly and A.L. Zydney, Effects of intermolecular thio-sulfide interchange reactions on BSA fouling during microfiltration, *Biotechnology and Bioengineering* 1994, *44*, 972-982.
[39] A.G. Fane, Ultrafiltration: Factors influencing flux and rejection, In Progress in Filtration and Separation; Edited by R.J. Wakeman, Elsevier Science Publishers, The Netherlands, 1986, Vol. 4, 101-179.
[40] W.R. Bowen and Q. Gan, Properties of microfiltration membranes : Flux loss during constant pressure permeation of bovine serum albumin, *Biotechnology and Bioengineering* 1991, *38*, 688-696.
[41] C.J.D. Fell, K.J. Kim, V. Chen, D.E. Wiley and A.G. Fane, Factors determining flux and rejection of ultrafiltration membranes, *Chem. Eng. Process.* 1990, *27*, 165 –173.
[42] B. Chaufer, J. Dulieu and B. Sebille, Modification de l'adsorption des protéines et du colmatage de membranes inorganiques d'ultrafiltration modifiées par dépôt de polymères fonctionnalisés, Proceeding of the First International Conference on Inorganic Membranes (ICIM), Montpellier (France), July 3-6, J. Charpin and L. Cot Eds., 1989, 135-140.

[43] M. Cheryan and U. Merin, A study of the fouling phenomenon during ultrafiltration of cottage cheese whey, in A.R. Cooper (Ed.), Ultrafiltration Membranes and Applications, Plenum Press, New York, 1980, pp. 619-630.
[44] M. Turker and J. Hubble, Membrane fouling in a constant-flux ultrafiltration cell, *J. Membrane Sci.* 1987, *34*, 267-281.